Journal of Catalysis 323 (2015) 45–54

Contents lists available at ScienceDirect

Journal of Catalysis

journal homepage: www.elsevier.com/locate/jcat

Heterogeneous complexes of nickel MCM-41 with β-diimine ligands: Applications in olefin oligomerization

Enéderson Rossetto [a], Bruna Pes Nicola [b], Roberto Fernando de Souza [b,1], Katia Bernardo-Gusmão [b], Sibele B.C. Pergher [a,*]

[a] LABPEMOL, Institute of Chemistry, Universidade Federal do Rio Grande do Norte-UFRN, Campus universitário, Lagoa Nova, 59078-970 Natal, RN, Brazil
[b] Institute of Chemistry, Universidade Federal do Rio Grande do Sul-UFRGS, Av. Bento Gonçalves, 9500, P.O. BOX 15003, 91501-970 Porto Alegre, RS, Brazil

ARTICLE INFO

Article history:
Received 17 September 2014
Revised 21 December 2014
Accepted 22 December 2014
Available online 13 January 2015

Keywords:
Oligomerization
MCM-41
β-diimine
Nickel complex

ABSTRACT

The β-diimine ligands 2-(phenyl)amine-4-(phenyl)imine-2-pentene and 2-(2,6-dimethylphenyl)amine-4-(2,6-dimethylphenyl)imine-2-pentene were combined with the alkoxysilane group chloropropyltrimethoxysilane (CPTMS) and covalently anchored to a mesoporous MCM-41 support; they were ordered via interactions with the silanols of the silica matrix and complexed with nickel. The complexes were synthesized for use in ethylene and propylene oligomerization and for comparing the results of homogeneous and heterogeneous systems. The support was first synthesized, calcined, anchored to the ligand, and then, complexed with nickel. These materials were characterized using various techniques, such as ^{1}H, ^{13}C, and ^{29}Si NMR, small angle XRD, thermogravimetric analysis, adsorption isotherms, transmission electron microscopy, and flame atomic absorption spectroscopy, to confirm the success of the synthesis. Both homogeneous and heterogeneous complexes are active and selective for the reactions of ethylene and propylene oligomerization.

1. Introduction

The development of materials and methods for catalytic oligomerization of light olefins to give alpha-olefins, such as 1-butene and 1-hexene, is an important topic in the chemical industry [1]. In the current climate and for the environmental vision of the world, developing systems that are more efficient, economically viable, and less harmful to the environment is very important. In this context, heterogeneous systems and anchoring of homogeneous catalytic complexes on supports, such as alumina and silica [2], are very promising methods for reducing the use of organic solvents in the easy separation of the reaction medium, thus reducing the costs and environmental impact [3].

The most important heterogeneous catalysts use nickel for ethylene oligomerization and are based on inorganic porous materials. The major methods for the preparation of heterogeneous nickel catalysts for oligomerization include NiO or $NiSO_4$ on various inorganic supports, Ni-exchanged zeolites, mesoporous materials (MCM-41, Al-MCM-41), sulfated alumina, and silica–alumina [4–7]. However, when nickel complexes were heterogenized on inorganic supports (SiO_2 or Al_2O_3), a decrease in activity occurred in some cases, and increases in selectivity and catalyst stability were often observed in ethylene oligomerization reactions [8–10].

Nickel complexes are most commonly used for oligomerization reactions in homogeneous media because of their high activity and ability to form specific products. Therefore, they are highly successful both from an academic standpoint and in the industry, resulting in their use in various industrial processes [11–13]. The commercial oligomerization of ethylene is predominantly performed using transition metal catalysts that produce a wide distribution of linear alpha-olefins, which are used in polymerization and the preparation of a variety of economically important compounds, such as detergents, synthetic lubricants, plasticizers, and alcohols [1]. Propylene has been less well studied than ethylene as an active and selective catalyst for α-olefins; there are also problems with it regarding its dimer requirements and in obtaining products with the desired regioselectivity [14].

Highly active nickel complexes with diimine ligands for ethylene oligomerization or polymerization were introduced by Brookhart et al. [15–18]. After that, significant effort was put toward studying the effects of the structures of the ligands on the catalytic properties of the metal complexes involved in the oligo/polymerization [19–22]. β-diimines and β-diiminatos have been studied as ligands for transition metal compounds [23,24]. Some ligands, such

* Corresponding author.
E-mail address: sibelepergher@gmail.com (S.B.C. Pergher).
[1] In memoriam.

http://dx.doi.org/10.1016/j.jcat.2014.12.026
0021-9517/

as β-diimines, are easy to prepare and have several attractive proprieties, including tunable electronic and steric parameters [22]. In the case of β-diimine ligands, the presence of acidic protons in the α position facilitates their anchoring via covalent bonding to the inorganic supports.

Homogeneous catalysts usually contain uniform and well-defined active sites, which lead to high activities and reproducible selectivities. However, the major drawback of using these catalysts is the difficulty in separating the catalysts, products, and solvent. An alternative to circumvent this drawback is to immobilize the homogeneous catalyst in various media, including inorganic and organic supports [25–28].

In the1990s, a new family of porous materials, which present a system of well-defined mesopore sizes with a regular spatial arrangement, was discovered by scientists at Mobil [29]. This family is called M41S and is composed of three types of phases; one of this materials was called MCM-41. Mesoporous materials of the MCM-41 type are very interesting because they have ordered arrays of uniform channels, a high surface area, thermal and chemical stability, and shape selectivity. These materials have a large number of hydroxyl groups, which provide the necessary qualities for modification of the internal and external surfaces, and the possibility of the self-assembly of molecules; these properties provide excellent chemical aggregation via covalent complexation with homogeneous media [30]. The synthesis of mesoporous materials modified with reactive functional groups, such as amines, aldehydes, nitriles, phenyls, thiols [31,32], modifying organic groups (functional ligands), or organometallic complexes with silanol groups (CPTMS and CPTES), for anchoring via covalent bonding, has been well studied with promising results observed in the last decade [3,30]. These systems allow anchoring via covalent bonding between the silanol groups of the organic functional groups and the Si–OH groups of the mesoporous materials or between the functional groups of the modified mesoporous materials and organic groups of interest.

There are studies that use homogeneous nickel complexes of β-diimines for oligomerization of olefins [8,33–36]; however, there are no reports of studies using anchoring via covalent bonds between nickel complexes, β-diimines, and ordered mesoporous materials for the oligomerization of ethylene and propylene.

The objective of this study was to investigate the potential for developing new nickel complexes heterogenized on mesoporous materials via anchoring with covalent bonds between the MCM-41 mesoporous support and nickel complexes with β-diimine ligands, attempting to produce catalyst complexes that are active and selective for the oligomerization of olefins (ethylene and propylene).

2. Experimental section

All experiments were performed under an argon atmosphere using standard Schlenk techniques. The solvents were deoxygenated by refluxing over appropriate drying agents (toluene and ethyl ether on sodium benzophenone and dichloromethane and acetonitrile on phosphorous pentoxide) under argon and distilled immediately prior to use. Methanol and tetrahydrofuran (THF) were used without further purification. Aniline, 2,6-dimethylaniline, and hexadecyltrimethylammonium bromide (CTABr) were purchased from Sigma–Aldrich and distilled under reduced pressure prior to use. 3-chloropropyltrimethoxysilane (CPTMS), sodium aluminate, sodium hydroxide, tetramethyl ammonium hydroxide (TMAOH), sodium hydride (NaH), and anhydrous nickel bromide ($NiBr_2$) were purchased from Sigma–Aldrich. Silica Aerosil 200 was purchased from Degussa. *p*-Toluenesulfonic acid (Vetec) was distilled on toluene using the Dean–Stark technique. Sodium carbonate was purchased from Vetec and used without further purification. Ethylaluminum sesquichloride ($Al_2Et_3Cl_3$, EASC) was supplied by Akzo Nobel and used with toluene dilution (10%). The solids were dried under reduced pressure.

2.1. Characterization techniques

Elemental analyses were performed using a Perkin Elmer M CHN Analyzer 2400. The liquid ^{13}C NMR analyses were performed using a Varian Inova 400 MHz solubilized in deuterated chloroform ($CDCl_3$). The ^{13}C and ^{29}Si CP-MAS-NMR analyses were performed using an Agilent 500 MHz spectrometer model DD2 operated at 125.7 MHz for ^{13}C and 99.3 MHz for ^{29}Si using adamantine as a reference material for peak assignments. The solid NMR conditions are an acquisition time of 7 ms and a delay of 10 s with a rotation of 10 kHz to ^{13}C and an acquisition time of 9 ms and a delay of 5 s with a rotation of 5 kHz to ^{29}Si. Thermogravimetric analyses were performed on a TA Instrument TGA Q50. The samples were heated at 10 °C/min from 20 °C to 800 °C under nitrogen flow. The morphology and particle size of the products were investigated using an EVO50, Carl Zeiss scanning electron microscope (SEM) operating at 30 kV. For the TEM analysis, a JEOL JEM 2010 transmission model was used with an acceleration voltage of 200 kV. After sample pretreatment for 12 h at 90 °C, the specific surface areas of the samples were determined via nitrogen adsorption–desorption using a Micrometrics TriStar II 3020. X-ray diffraction analyses were performed on a Bruker D2 Phaser using Cu Kα radiation ($\lambda = 1.54$ Å) in the range $2\theta = 1°–8°$ using slits of 0.1 and 3 nm. The nickel content of the solids was determined via flame atomic absorption spectrometry (FAAS). The analysis was performed using a Perkin Elmer A atomic absorption spectrometer with a hollow nickel cathode lamp ($\lambda = 232$ nm) and air–acetylene flame (10 L/min: 2.5 L/min). The samples were prepared by treating 50 mg of the heterogeneous complex with 2 mL of HCl, 6 mL of HNO_3, and 5 mL of HF, adding the mixture to Teflon autoclaves and, subsequently, using a digester for 24 h at 150 °C. After cooling, the samples were diluted to 50 mL.

2.2. Synthesis of *L1* and *L2* ligands and homogeneous *C1* and *C2* nickel complexes

The syntheses and characterization of ligands **L1** = 2-(phenyl)amine-4-(phenyl)imine-2-pentene and **L2** = 2-(2,6-dimethylphenyl)amine-4-(2,6-dimethylphenyl)imine-2-pentene and their corresponding nickel complexes **C1** = dibromo(*N,N-bis*(phenyl)-2,4-pentanediimine)nickel(II) and **C2** = dibromo(*N,N-bis*(2,4-dimethylphenyl)-2,4-pentanediimine)nickel(II) were described in a previous work [8].

2.3. Synthesis of MCM-41

The syntheses of mesoporous MCM-41 materials were based on the synthesis described by Corma et al. [36]. The synthesized material has the following molar ratio: 1 SiO_2:0.1 CTABr:0.25 TMAOH:20 H_2O.

Solution A was added to a plastic beaker under heating at 40 °C and mechanical agitation with 134 g of distilled water and 20 g of CTABr. The solution was stirred for 1 h.

Solution B: In a plastic beaker, 34.6 g of TMAOH 25% and 3.84 g of aerosil silica were added and left under magnetic stirring for 45 min to homogenize the sample.

Subsequently, solution B was added to solution A under mechanical stirring and slowly added to 18.08 g of aerosil silica. The gel formed was left under stirring for 1 h to homogenize the sample (pH = 13). The resulting gel was transferred to 4 stainless steel autoclaves with Teflon slings and placed in a static oven at

135 °C for 24 h. The resulting material was filtered with distilled water and then dried at 100 °C for 4 h. Subsequently, the material was calcined at 550 °C for 6 h under nitrogen and synthetic air yielding 15.36 g of calcined MCM-41.

2.4. Synthesis of the hybrid mesoporous materials

The hybrid mesoporous materials were synthesized based on previously published methods [8]. This method requires the completion of four successive steps:

1. *Activation of ligand*
2. *Synthesis of organic precursor*
3. *Anchoring of the organic precursor*
4. *Complexation of nickel*

2.4.1. Activation of the ligand: synthesis of the sodium salt

The ligand (6 mmol) was activated with sodium hydride NaH (9 mmol) using dichloromethane (20 mL) as the solvent, as is shown in step 1 in Fig. 1. This reaction was monitored by the liberation of H_2. The mixture was left under stirring for 30 min under an inert atmosphere at a temperature of 35 °C. The solvent was removed under reduced pressure.

2.4.2. Synthesis of silylated organic precursor

A solution of 1.1 mL (6 mmol) of CPTMS in 5 mL of toluene (THF) (1:1) was added to sodium salt under an argon atmosphere. The mixture was stirred and refluxed at 80 °C for 3 h. The resulting solution was centrifuged to separate the produced NaCl, the excess NaH, and the supernatant containing the organic ligand precursor, which is used in the synthesis of the hybrid xerogel. Step 2 in Fig. 1 shows the synthesis reaction of the organic precursor.

2.4.3. Anchoring of the L1 and L2 ligands

In this method, the mesoporous supports are first synthesized and calcined at 540 °C for 6 h under airflow. The support of MCM-41 was calcined and pre-treated at 100 °C for 6 h under high vacuum. This procedure was used to remove residual moisture from the support. This step was performed after the synthesis of the silylated organic precursor using the ligand in a reaction with NaH followed by reaction with CPTMS. The silylated organic precursor coupled with the support was combined with toluene and left for 24 h at 80 °C under reflux, as shown in step 3 of Fig. 1.

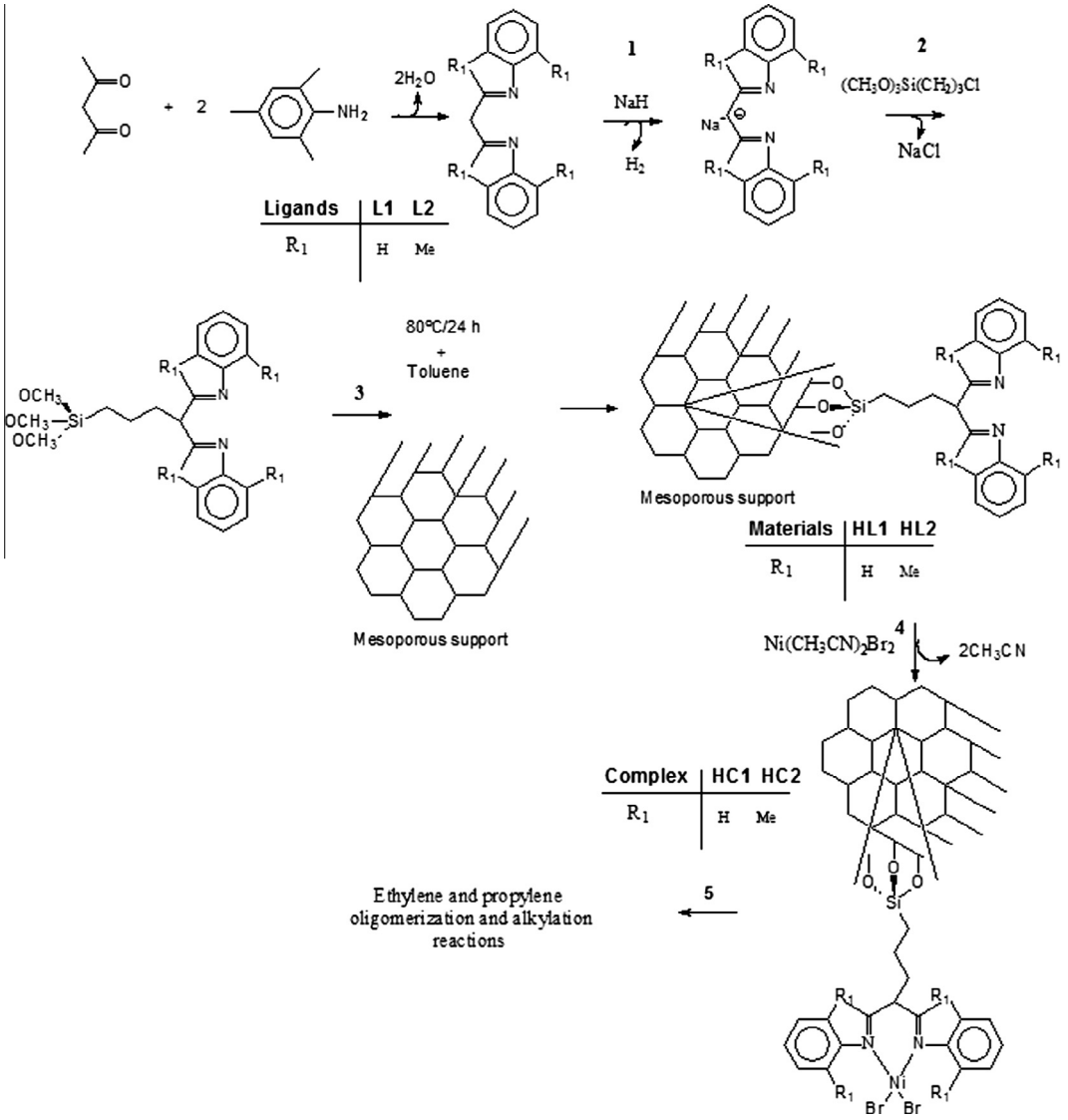

Fig. 1. Anchoring via covalent attachment of **L1** and **L2** in MCM-41 and obtaining the heterogeneous complexes **HC1** and **HC2**.

The solid phase was filtered and washed with dichloromethane to remove the un-anchored ligands and then dried under vacuum. All procedures were performed under an argon atmosphere.

2.4.4. Complexation of nickel

2.4.4.1. Synthesis of the $Ni(CH_3CN)_2Br_2$ adduct. The synthesis of the adduct was performed according to Hathaway et al. [37]. In a Schlenk flask, 4.981 g (22.8 mmol) of $NiBr_2$ was added to 240 mL of acetonitrile. The reaction mixture was left under stirring and refluxing conditions for 4 h at 80 °C, forming a blue oil solution. The mixture was concentrated to 20 mL. A light yellow solid was obtained, which was filtered, washed with acetonitrile, and dried under argon flow. The mass of the product was 6.012 g, with a yield of 87.9%. $Ni(CH_3CN)_2Br_2$ adduct was used in the synthesis of the diimine nickel complexes.

2.4.4.2. Complexation of nickel. These complexes are used as catalyst precursors for the oligomerization reactions of ethylene and propylene in heterogeneous media. In a Schlenk flask, 1.2 equivalents of $Ni(CH_3CN)_2Br_2$ were added with respect to the amount of ligand calculated via elemental analysis of CHN, and 20 mL of dichloromethane was then added to the hybrid materials **HL1** and **HL2**, as shown in step 4 of Fig. 1. This suspension remained under agitation for 5 days at room temperature. Upon completion of the synthesis, the suspension was filtered using a Schlenk filter and washed with acetonitrile until the solvent was clear (approximately four 30-mL aliquots). The **HC1** and **HC2** solids obtained were dried under reduced pressure and submitted for analysis using FAAS.

2.5. Ethylene oligomerization runs

The reactions were performed in homogeneous and heterogeneous phases, and the results were compared.

The oligomerization reaction experiments were performed in a 450-mL Parr stainless steel autoclave equipped with a magnetically driven mechanical stirrer, a thermocouple, and a pressure gauge. The reaction temperature (10 °C) was controlled using a thermostatic bath.

In a typical homogeneous or heterogeneous reaction run, a solution of EASC and 60 mL of toluene was added to the reactor under argon, followed by the addition of 20 μmol or 13 μmol of the catalytic precursor. The reactor was pressurized with ethylene or propylene, and the temperature was adjusted to 10 °C using thermostatic bath circulation. The Al/Ni molar ratios varied from 100 to 200, and the ethylene or propylene pressure was 15 atm and 5 atm, respectively. After 30 min, the reaction was stopped, and the mixture was cooled to −30 °C for ethylene and 10 °C for propylene and analyzed immediately using gas chromatography.

Recycle experiments were performed in a 100-mL double-walled glass reactor containing a magnetic stirring bar with a constant supply of neat gaseous propylene at 6 atm and a thermocouple to measure the temperature. The reaction temperature was held at 10 °C using an external-circulation ethanol bath. In a typical experiment, the reactor was charged with a solution of the desired catalytic precursor (13 μmol) in 60 mL of toluene saturated with propylene. The reactor was purged with propylene, and the alkylaluminum solution was added in the amount needed to obtain an aluminum to nickel molar ratio (Al/Ni) of 200. After 30 min, the reaction was stopped, and the mixture was cooled and analyzed using gas chromatography. After the first reaction, the products were removed from the reactor through a cannula. The catalyst recycling was accomplished by adding another 50 mL of toluene and 4.6 mL of EASC and continuing the reaction.

In all cases, the chromatographic analyses were performed using a Shimadzu GC-2010 gas chromatograph equipped with a Petrocol DH capillary column (methyl silicone, 100 m in length, 0.25 mm ID, 0.5 μm film thickness). The analysis conditions for ethylene were 36 °C for 15 min, followed by heating at a rate of 5 °C/min to 250 °C. For propylene, the analysis conditions were 36 °C for 30 min, followed by heating at a rate of 5 °C/min to 250 °C. The products were identified using the method of co-injection of standards, and isooctane was used as the internal standard for quantification. The TOF values, defined as moles of converted ethylene per mole of pre-catalyst per reaction time (in h), show a variation of ±10%, as determined by at least three independent experiments performed under each condition.

3. Results and discussion

The ability of these complexes to anchor via covalent bonding with the silanol matrix silica allows for the transformation of a homogeneous system to a heterogeneous system, realizing many advantages by combining two different materials, for example, easy separation from the reaction medium and the ability to reuse and recycle the complex.

The anchoring of complexes **C1** and **C2** was developed at different stages via functionalization of the ligand and its interaction with the silanol support, as demonstrated in Fig. 1, and the complexes were characterized using various analytical techniques to confirm the success of the synthesis and evaluate the characteristics of the materials. Fig. 2 shows the XRD patterns of the calcined MCM-41 after anchoring of the ligands **HL1** and **HL2** and after metal complexation of **HC1** and **HC2**. In the diffractogram of the calcined sample, the presence of three reflections can be observed (Miller indices (100), (110), and (200)) in the region of $2\theta = 2°–8°$. The characteristics of the MCM-41 mesoporous materials are a typical hexagonal structure and a good ordering of the mesopores,

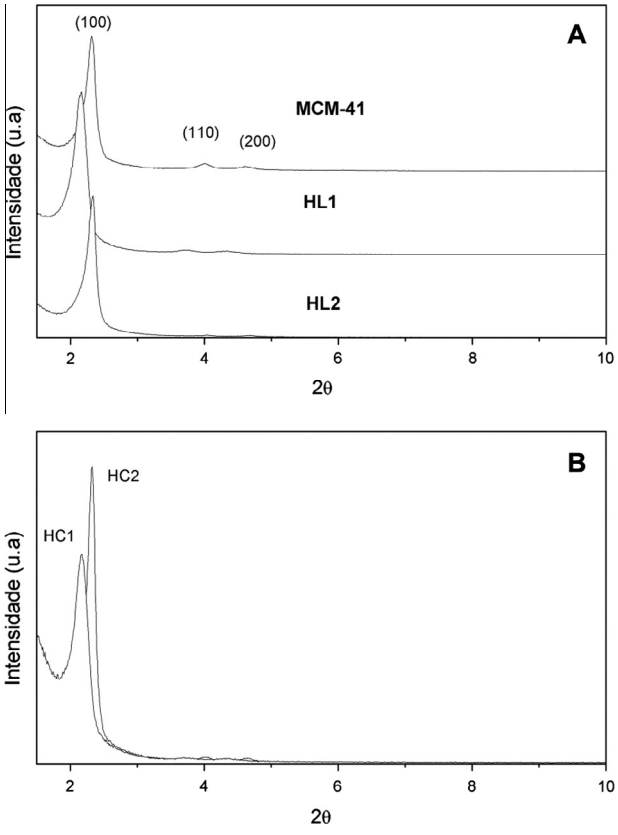

Fig. 2. XRD pattern of (A) calcined MCM-41, **HL1** and **HL2,** and (B) **HC1** and **HC2**.

which can be confirmed by analyzing the transmission images shown in Fig. 7. The diffractogram of the sample after anchoring of the ligand and nickel complexation shows reflection characteristics of the MCM-41 mesoporous materials, but the reflections (110) and (200) have a lower intensity, which may be due to the anchoring of the organic matter and the complexation of the metal. These characteristics may distort the regular matrix of MCM-41 or interfere with the X-ray analysis. This small decrease in intensity is not interpreted to be a severe loss of long-range ordering in the silica structure [38,39].

N_2 adsorption–desorption isotherms of calcined MCM-41 and the samples after the anchoring of L1 and L2 ligands are shown in Fig. 3. We can observe a typical type IV isotherm of mesoporous materials (defined using IUPAC) with a type 1 hysteresis [40]. The results of the texture analysis from the N_2 adsorption–desorption isotherms are shown in Table 1. Calcined MCM-41 has a BET area of 1009 m^2/g and a mesopore volume of 0.98 cm^3/g. The **HL1** and **HL2** materials exhibit decreases in the BET area of 691 and 698 m^2/g and mesopore volume of 0.60 and 0.58 cm^3/g, respectively. The values of the pore sizes of the materials (MCM-41 calcined, 2.71 nm) changed after the anchoring of the **L1** (2.48 nm) and **L2** (2.35 nm) ligands. The relative pressure where the pores of the materials are filled is shifted to lower values for the **HL1** and **HL2** samples compared to the source material, calcined MCM-41, resulting in a decrease in the BET surface area, pore volume, and pore diameter, indicating that the anchored organic matter (**L1** and **L2**) is within the pores of the MCM-41.

Using XRD and gas adsorption analyses, we can calculate the lattice parameters of the unit cells (a_0), the wall thicknesses (W_t), and the pore diameters (D_p) of these materials. The results are shown in Table 1. After the anchoring of the **L1** and **L2** ligands, the pore size decreased and the wall thickness increased, indicating that the ligands are within the pores of the MCM-41 material and connected to the walls, which is in agreement with the values obtained from the adsorption–desorption isotherms.

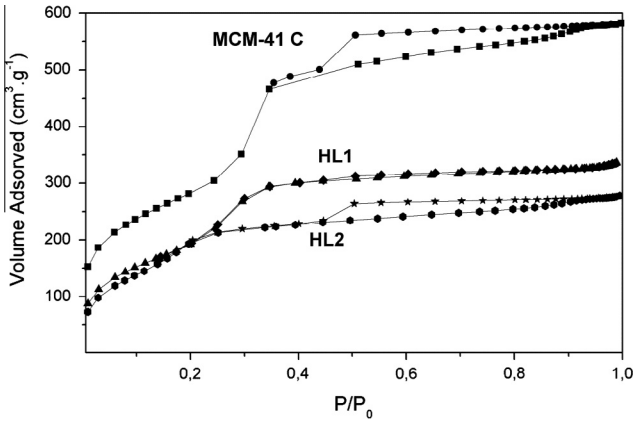

Fig. 3. Adsorption–desorption isotherms of calcined MCM-41, **HL1** and **HL2**.

The solution ^{13}C NMR spectrum of L1 and solid ^{13}C and ^{29}Si NMR spectra of HL1, which were chosen to represent the results after the anchoring of the ligands, are shown in Fig. 4. In the solution ^{13}C NMR spectrum of **L1,** the signals were assigned (Fig. 4A) and we can observe that the more intense signals are the aromatic ones (122, 123, and 128 ppm). After anchoring the ligand **L1** (Fig. 4B), we can assign the signal at 7.9 ppm to the carbon attached to the silicon in MCM-41. The signals at 24.8 and 48.3 ppm are attributed to methyl carbon and carbon bound to the **L1** ligand [30]. The only three signals of the ligand that can be observed are the aromatics carbons. The aliphatic ones related to the ligand cannot be observed perfectly due to the high noise level of the analysis and the excess of fixed propyl from chloropropyltrimethoxysilane. Fig. 4C shows the ^{29}Si NMR analysis of the calcined MCM-41, and we can observe the NMR signals at 94 ppm assigned to the group Q^2 [germinal silanol, $(SiO)_2Si(OH)_2$], Q^3 at 101 ppm [single silanol, $(SiO)_3Si(OH)$], and Q^4 at 109 ppm [siloxane, $(SiO)_4$ Si], showing the silica sites of the structure [30]. After the anchoring of the **L1** and **L2** ligands, the intensity of the signal from silicon Q^2 is reduced considerably (94 ppm), but the signals for Q^3 (101 ppm) and Q^4 (109 ppm) increase in intensity, which is due to the consumption of Si–OH and $Si(OH)_2$; this result can also be observed in the infrared spectrum because the band related to the Si–O–Si bond in the **HL1** and **HL2** samples increases to 1050 cm^{-1} compared to the MCM-41 matrix. In the **HL1** ^{29}Si NMR sample**,** the appearance of two resonance signals at 60 ppm is also observed, which are assigned to the group T^2 [C–$Si(OSi)_2$(OH)], and at 68 ppm, which are assigned to the group T^3 [C–$Si(OSi)_3$] [30]. From the results of the ^{13}C and ^{29}Si NMR, we can say that the **L1** and **L2** ligands are successfully anchored via covalent Si–O–C bonds to the MCM-41, and together with the XRD results and adsorption–desorption isotherms of these materials, we see that they are preferably within the pores of the MCM-41, maintaining a regular structure with characteristic hexagonal ordered materials. The heterogenized nickel complexes **HC1** and **HC2** were not subjected to ^{13}C and ^{29}Si NMR analysis due to the paramagnetic metal.

The elemental analysis and flame atomic absorption (FAAS) data (see Table 1) were used to determine the ligand incorporation percentage and quantify the organic matter attributed to **L1** and **L2** anchored to the MCM-41 matrix and to quantify the nickel in **HC1** and **HC2** (see Table 1). The analysis of the N content reveals that

Table 1
Structural properties of the synthesized materials.

Sample	d_{100} (nm)	a_0[a] (nm)	A_{BET}[b] ($m^2\ g^{-1}$)	V_{total}[c] ($cm^3\ g^{-1}$)	V_{meso}[d] ($cm^3\ g^{-1}$)	D_p[e] (nm)	W_t[f] (nm)	Ligand incorporation (%)[g]	Organic content (μmol/g)[g]	Nickel content[h] (μmol/g)
MCM-41 Calcined	3.80	4.39	1009 ± 10	0.98	0.98	2.71	1.68	0.0	0.0	0.0
HL1	4.07	4.70	691 ± 15	0.60	0.60	2.48	2.22	17	124	130 ± 1.87[i]
HL2	3.82	4.41	698 ± 36	0.53	0.53	2.35	2.06	11	175	159 ± 0.85[j]

[a] a_0: lattice parameter in the unit cell = $2d100/\sqrt{3}$.
[b] A_{BET} = specific area obtained using the BET method (total area).
[c] V_{total} = total pore volume obtained for P/P_0 = 0.98 using the rule of Gurvich.
[d] V_{meso} = pore volume related to the contribution of mesopores obtained using BJH method.
[e] D_p = average pore diameter calculated by intervals obtained using the BJH desorption method.
[f] W_t: Wall thickness = a_0–D_p.
[g] Ligand incorporation and organic content: calculated from the %N obtained from the elemental analysis.
[h] Nickel content of complexes **HC1**[i] and **HC2**[j].

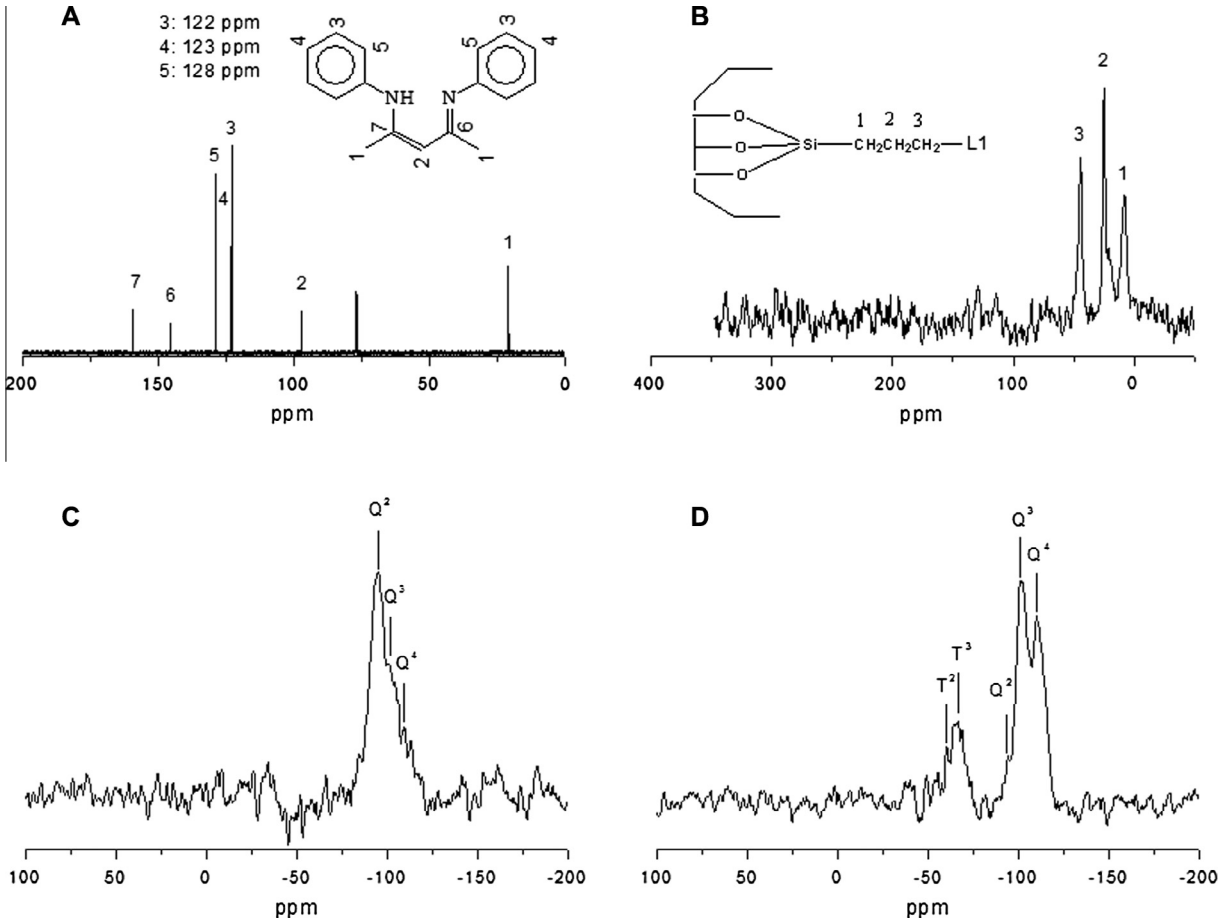

Fig. 4. ^{13}C NMR spectra of, (A) Homogeneous **L1**, (B) **HL1** ^{29}Si NMR spectrum of (C) calcined MCM-41, and (D) **HL1**.

the amount of organic material anchored to the MCM-41 matrix was 17% and 11% of the 6 mmol added. These correspond to 124 μmol/g (36 mg/g) for **HL1** and 175 μmol/g (61 mg/g) for **HL2**. The amount of active sites of heterogeneous complexes **HC1** and **HC2** was calculated based on the concentration of nickel (7.84 mg/g **HC1** and 9.34 mg/g **HC2**) obtained using FAAS. These quantities correspond to about one nickel for each ligand (130 μmol/g and 159 μmol/g).

Thermograms of calcined MCM-41 and the **HL1** and **HL2** hybrid materials are shown in Fig. 5A. In the calcined MCM-41, water mass loss occurred at temperatures below 150 °C. For the **L1** and **L2** ligands, as shown in Fig. 5B, the decomposition temperature of the organic material occurs between 130 and 270 °C, with a degradation peak at 280 °C. After anchoring in the silica matrix (**HL1** and **HL2**), the TGA curves show loss of adsorbed water, structural desidroxilation, methanol loss from methoxy groups, and residual solvent (toluene) and organic material decomposition. The temperature range of the decomposition increases from 150 to 400 °C with a decomposition peak at 380 °C, indicating that the material is more resistant to temperature effects, which is attributed to covalent ligand anchoring on the MCM-41 matrix. From NMR results, elemental analysis and TGA, it can be argued that the ligands were anchored successfully at the MCM-41 matrix.

Scanning electron microscopy was performed with the aim of evaluating the morphology of the materials before and after anchoring of the ligands, which is shown in Fig. 6. We can observe the morphology of the particle agglomerates with irregular sizes, which are usually observed in MCM-41 [41]. After anchoring of the **L1** and **L2** ligands, no change in the morphology of the material is observed.

Fig. 7 shows transmission electron microscopy (TEM) images. A) image viewed along the [0 1 0] axis, and B) image viewed along the [1 0 0] axis. In the TEM images, mesoporous channels in a hexagonal arrangement with good order can be observed.

Homogeneous complexes **C1** and **C2** and the heterogeneous complexes **HC1** and **HC2** were combined with EASC and used as catalysts for the oligomerization reaction of ethylene and propylene. The results in homogeneous media, as previously described [8], were compared with those obtained in heterogeneous media. All reactions were performed at least in duplicate. Both homogeneous complexes and heterogeneous complexes were active in the oligomerization reaction. The reaction parameters of temperature (10 °C), Al/Ni ratio, reaction time, and ethylene pressure were studied in the previously described works [8,42].

The results of the oligomerization of ethylene are shown in Table 2. Entries 1 and 2 are related to the homogeneous complex. The **C1** complex without substituents on the phenyl ring had a higher activity ($210.0 \times 10^3\ h^{-1}$), with selectivity for the C_4 fraction of 78%, which were comparable with the **C2** complex with substituents on the phenyl ring, but the **C2** complex had greater selectivity for the C_4 fractions (97%). These results suggest that the greater steric hindrance of the methyl groups decreases the accessibility of the ethylene and, consequently, reduces the activity of the reaction. This behavior is predominantly related to electronic effects [8,43].

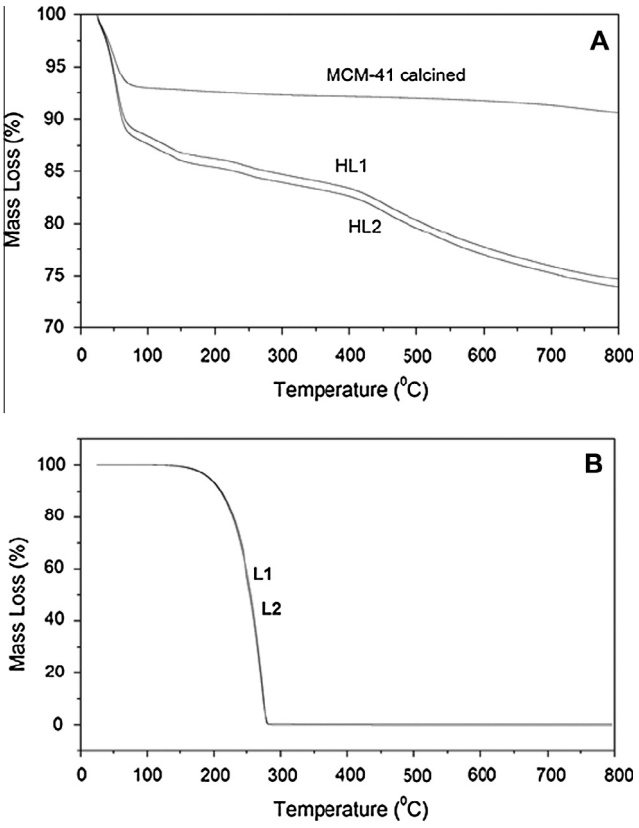

Fig. 5. Thermogravimetric analysis of (A) calcined MCM-41, **HL1** and **HL2** materials, and (B) **L1** and **L2** ligands.

Entries 3 and 4 are related to reactions in heterogeneous media. Thirteen μmol of the complex, determined based on the amount of nickel incorporated in the material, was used, assuming that all metal species are active. An Al/Ni ratio of 200 for the reactions in heterogeneous media was used. The **HC1** complex has a greater activity of $18.1 \times 10^3\ h^{-1}$ compared with **HC2** ($12.7 \times 10^3\ h^{-1}$) and has the same selectivity for the C_4 fraction (97% and 98%, respectively). However, the selectivity for the α-C_4 fraction by the **HC2** complex (90%) is higher than for the **HC1** complex (76%). This behavior may be related to the greater steric hindrance of the **HC2** complex, which possesses two methyl groups at the ortho position of the phenyl.

The results from the homogeneous complex entries 1 and 2 were compared with the results of the heterogeneous complex entries 3 and 4. As described in Table 2, Al/Ni = 200. It is necessary to use a larger amount of the complex to activate the alkylaluminum due to the presence of hydroxyl groups in the MCM-41 matrix, which consumes alkylaluminum [8]. The heterogeneous complex entries 3 and 4 showed a lower catalytic activity for ethylene oligomerization than the homogeneous analogue inputs 1 and 2, most likely because of the heterogeneous catalysts having a lower number of active species, which is related to the need to use a greater amount of alkylaluminum to activate the Ni species due to the presence of hydroxyls.

Heterogenized complexes exhibited a lower activity for oligomerization of ethylene. However, the heterogenized complexes exhibited the best selectivities for both C_4 and α-C4 fractions compared with homogeneous complex **C1.** Heterogenized complex **HC2** exhibited the same selectivity as the analogous homogenous complex. MCM-41 serves as a support for the catalysts and acts as a steric hindrance for the formation of internal olefins.

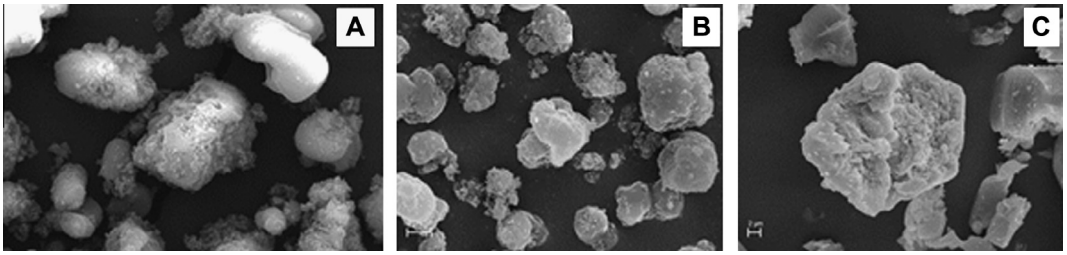

Fig. 6. Micrographs of (A) calcined MCM-41, (B) **HL1** and (C) **HL2**.

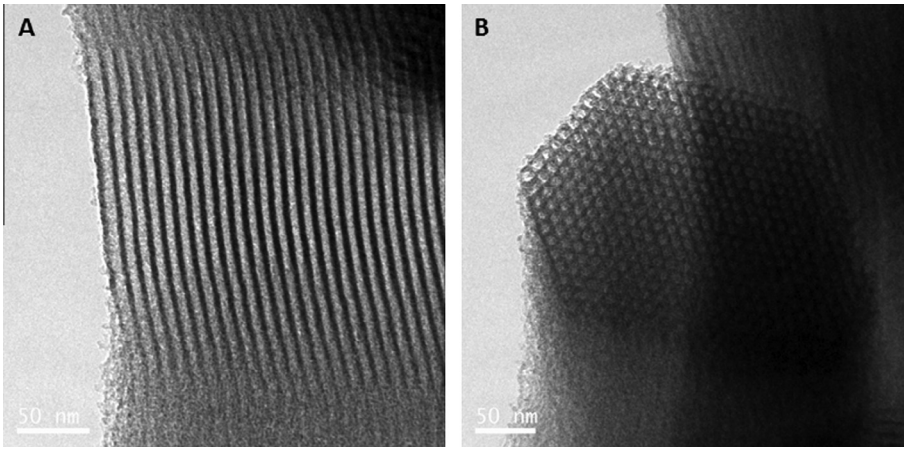

Fig. 7. Transmission electron microscopy of calcined MCM-41. (A) Image viewed along the axis [010] and (B) image viewed along the [100] axis.

Table 2
Results of the ethylene reactions of homogenous and heterogeneous nickel complexes.

Entry	Complex	Al/Ni	TOF (10^3 h^{-1})	Sc_4 (%)	α-c_4 (%)	Sc_6 (%)
1	C1	100	210.0	78	32	20
2	C2	100	18.3	97	87	3
3	HC1	200	18.1	97	76	3
4	HC2	200	12.7	98	90	2

Complex: 20 μmol for homogeneous and 13 μmol for heterogeneous, pressure: 15 atm of ethylene, T = 10 °C, time = 0.5 h, solvent = toluene (60 mL), cocatalyst = EASC.

The results of the oligomerization of propylene for homogeneous and heterogeneous complexes are shown in Table 3. The same reaction conditions were used as in the oligomerization of ethylene, but for propylene, the maximum usable pressure is 6 atm. The behavior of the homogeneous and heterogeneous complexes used for the oligomerization of propylene was studied, and the results were compared for the two systems. All complexes were active for the oligomerization of propylene. When toluene was used as the solvent, the reaction product was the alkylation of toluene with propylene after a reaction called Friedel–Crafts alkylation [44–51]. The product obtained is considered a parallel reaction to propylene oligomerization. To avoid this unwanted product, cyclohexane was tested as the solvent in the reaction.

The homogeneous complex inputs 1 and 2 (Table 3) were active for the oligomerization of propylene, resulting in activities of 105×10^3 h^{-1} for the **C1** complex and 42×10^3 h^{-1} to the **C2** complex, and presenting low activity for toluene alkylation of 1.6 and 0.9×10^3 h^{-1}, respectively. A selectivity of 98% was obtained for the C_6 products, and 53% was obtained for linear C_6 using complex **C1** and 30% using complex **C2**.

The **HC1** and **HC2** heterogeneous complexes**,** entries 3 and 4 in Table 3, showed quite different behavior compared with their homogeneous analogues, showing greater activity for the alkylation of toluene: 90×10^3 h^{-1} for **HC1** and 10×10^3 h^{-1} for **HC2**. This behavior, which favors the formation of alkylation products of toluene, is possibly related to the high Lewis acidity [52] of the species formed by the reaction of acidic groups on the surface of MCM-41 with the EASC co-catalyst.

Blank tests **B1**, **B2,** and **B3,** entries 7, 8, and 9 in Table 4, were performed to evaluate this behavior. Input 8 describes the **B2** test using the calcined MCM-41 without the complex and anchored with the EASC cocatalyst, resulting in an alkylation activity of 5×10^3 h^{-1}. This result was compared with input 7, test **B1**, which only uses the co-catalyst EASC, and has an alkylation activity of 2×10^3 h^{-1}. Entry 9, which has only the **B3** complex, uses the calcined MCM-41 and does not exhibit any catalytic activity. These behaviors explain the influence of the MCM-41 matrix on the catalytic activity for alkylation: it is more active when the MCM-41 and the EASC co-catalyst are combined, indicating that the

Table 3
Results of the oligomerization of propylene using the homogenous and heterogeneous nickel complexes.

Entry	Complex	n_{Ni} (10^{-6} mol)	Al/Ni	FRolig[a] (10^3 h^{-1})	FRalq[b] (10^3 h^{-1})	% Products					% C_6 linear[e]
						C_6[c]	C_9[c]				
	Homogeneous tests										
1	C1	20	100	105	1.6	98	0	1	0	1	53
2	C2	20	100	42	0.9	98	0	1	0	1	30
	Heterogeneous tests with toluene										
3	HC1	13	200	3	90	3	0	42	19	36	13
4	HC2	13	200	2	10	32	0	20	9	39	18
	Heterogeneous tests with cyclohexane										
5	HC1	13	200	2	0	100	0	0	0	0	29
6	HC2	13	200	4	0	100	0	0	0	0	30

Reaction conditions: time = 30 min, temperature = 10 °C, relations. Al/Ni = 100 and 200, cocatalyst = EASC, and propylene pressure = 6 atm.
[a] TOF oligomerization: mol of propylene oligomerized/(mol Ni * hours).
[b] TOF alkylation: mol of converted toluene/ (mol Ni * hours).
[c] Oligomerization products.
[d] Mono-(C10), di-(C13), and tri alkylation (C16) of toluene with propylene.
[e] % Calculated taking into account only the products of dimerization C_6.

Table 4
Results of the blank tests.

Entry	Complex	n_{Ni} (10^{-6} mol)	FRolig[a] ($10^3 h^{-1}$)	FRalq[b] ($10^3 h^{-1}$)	% Products					% C_6 linear[e]
					C_6[c]	C_9[c]				
7	B1 (EASC)	0	0	2	0	0	25	15	60	0
8	B2 (EASC/M-41)	0	0	5	0	0	43	15	41	0
9	B3 (M-41)	0	0	0	0	0	0	0	0	0

Reaction conditions: time = 30 min, temperature = 10 °C, and propylene pressure = 6 atm.
[a] TOF oligomerization: mol of propylene oligomerized/(mol Ni * hours).
[b] TOF alkylation: mol of converted toluene/ (mol Ni * hours).
[c] Oligomerization products.
[d] Mono-(C10), di-(C13), and trialkylation (C16) of toluene with propylene.
[e] % Calculated taking into account only the products of dimerization C_6.

Table 5
Distribution of the products of interest (C_6) from propylene oligomerization reactions in homogeneous and heterogeneous media.[a]

Entry	Complex	4M1P	2,3DM1B	c4M2P	t4M2P	2M1P	1H	t3H	t2H	2M2P	c2H	2,3DM2B
1	C1	1.3	5.3	35.3	4.1	–	4.3	15.7	28.1	–	4.0	1.8
2	C2	3.1	8.2	55.8	2.9	–	2.5	17.3	4.9	–	4.9	0.4
3	HC1	24.9	5.2	56.3	–	–	2.1	0.9	9.2	–	1.4	–
4	HC2	16.3	7.1	50.1	–	–	2.0	14.5	4.8	–	5.2	–
5	[a]HC1	19.1	7.1	41.7	2.7	2.2	1.3	14.2	4.3	–	6.5	0.9
6	[a]HC2	13.4	6.7	45.8	4.2	1.2	1.3	13.9	8.4	–	5.1	–

[a] Reactions performed with cyclohexane solvent. 4M1P (4-methyl-1-pentene), 2,3DM1B (2,3-dimethyl-1-butene), c4M2P (cis-4-methyl-2-penteno), t4M2P (trans-4-methyl-2-penteno), 2M1P (2-methyl-1-penteno), 1H (1-hexene), t3H (trans-3-hexeno), t2H (trans-2-hexene), 2M2P (2-methyl-2-pentene), c2H (cis-2-hexene), 2,3DM2B (2,3-dimethyl-2-butene).

Table 6
Distribution of products from alkylation reactions of oligomerization of propylene in homogeneous and heterogeneous media.

Entry	Complex	Selectivities for cymenes					
			Meta-cymene	Para-cymene	Ortho-cymene		
1	C1	1	18.3	33.4	48.3	0	0
2	C2	1	16.4	35.0	48.6	0	1
3	HC1	42	17.4	35.2	47.5	19	36
4	HC2	20	17.0	35.5	47.5	9	39
7	B1	43	16.1	32.6	51.3	20	47
8	B2	33	16.5	34.1	49.5	15	41

[a] Distribution of products in the range of C_{10}.

material has a certain acidity that directs the reaction to the formation of alkylation products.

The heterogeneous complexes **HC1** and **HC2** also have catalytic activities for C_6 products of $3 \times 10^3\ h^{-1}$ and $2 \times 10^3\ h^{-1}$ with selectivities of 13% and 18% for C_6 linear products, respectively. These homogeneous complexes are preferentially active for products in the range of C_6, with a small activity for the alkylation of toluene. The heterogeneous complexes exhibited activity for toluene alkylation products with a small activity for products in the range of C_6. The blank tests (**B1**, **B2,** and **B3**) showed only products for alkylation of toluene, with lower activity than the homogeneous and heterogeneous complexes, indicating the importance of the metal center for this type of reaction system.

Because the goal was to obtain products in the range of C_6, catalytic tests were performed using cyclohexane as a solvent, with no intention of obtaining alkylation products. We can see that entries 5 and 6, for heterogeneous complexes **HC1** and **HC2**, are active in the oligomerization of propylene and are selective for products in the range of C_6 (100% C_6, 30% linear). The catalytic activities shown in comparison with systems that use toluene as a solvent are lower. This observed decrease in activity was attributed to the lower solubility of propylene when in cyclohexane.

Table 5 shows the products obtained in the range of C_6 for the reaction of propylene oligomerization, both in homogeneous and in heterogeneous media for the two systems with different solvents. The products are branched in all cases, wherein the product obtained is c4M2P, showing that the second insertion of propylene occurs primarily at the two carbons, and the expected values of p and q were obtained.

In Table 6, the products of alkylation of toluene are shown. We observed products in the range of C_{10}, C_{13}, C_{16}, and C_{10}, with a distribution of products in meta-, para-, and ortho-cymene. All complexes exhibit almost the same behavior with respect to the distribution of products in the range of C_{10}. Heterogeneous complexes have the same behavior compared to each other and tend to produce more alkylation than their homogeneous analogues.

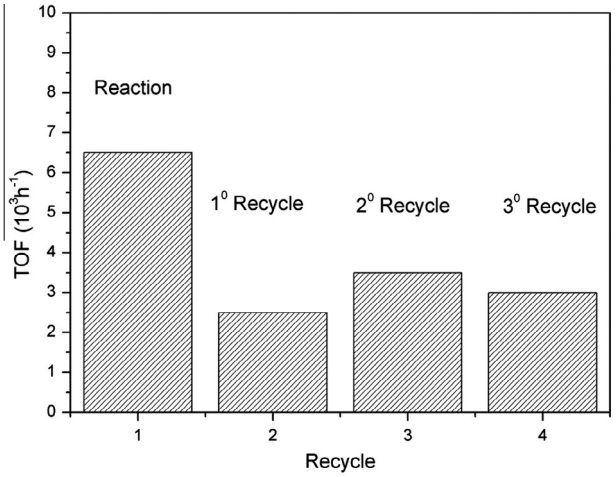

Fig. 8. Results of the **HC1** catalyst recycle reaction.

Recycle reactions (see Fig. 8) were performed using the heterogenized **HC1** complex, which was shown to be active in recycle reactions and is, therefore, promising for large-scale use. A decrease in the reaction activity compared to the first cycle is observed while remaining practically unchanged until the third cycle.

4. Conclusions

In this work, the oligomerization of ethylene and propylene catalyzed by homogeneous nickel diimine complexes and heterogeneous complexes combined with ethyl aluminum sesquichloride was studied. The influences of the structures of the ligands and the anchoring of ligands via covalent bonding on the activity and selectivity of the oligomerization were studied on an ordered MCM-41 support.

Heterogeneous compounds were obtained via modification of the ligands with chloropropyltrimethoxysilane and anchored via covalent bonds with the silica matrix via O–Si–O–Si–C connections, confirmed using solid-state ^{13}C and ^{29}Si NMR and infrared spectroscopy. The XRD patterns confirmed that the structure of MCM-41 remained in an ordered hexagonal form with a small reduction of the (110) and (200) reflections after the anchoring of the ligands. A decrease in the values of the area calculated using the BET method and a reduction in the pore volume after anchoring of the ligand in the material were observed via N_2 adsorption–desorption analysis, indicating that the organic material is preferably anchored within the pores of the MCM-41.

Both the homogeneous and heterogeneous complexes are active in oligomerization reactions. The reactions of ethylene with heterogeneous complexes were less active than their homogeneous analogues; however, they were more selective for both $C_4$and α-C_4 fractions. The addition of silica served as a support for the complexes and also acted as a steric hindrance, preventing the formation of internal olefins.

In the propylene oligomerization reactions, totally unexpected results were obtained when using toluene as a solvent in the reactions with heterogeneous complexes. The homogeneous complexes produced nearly the same range of C_6 olefins, and the heterogeneous complexes produce practically only alkylation products. Products in the range of C_6 for both homogeneous and heterogeneous complexes are preferably branched, and higher production was obtained from c4M2P. The products obtained from the alkylation of toluene with heterogeneous complexes can be explained by the contribution from the Lewis acidity of the MCM-41 support, as determined from the blank testing.

Propylene oligomerization reactions using cyclohexane as a solvent were performed. The products were only in the range of C_6. The reactions were less active than reactions using toluene as a solvent, most likely due to the lower solubility of propylene in cyclohexane.

Recycle reactions were performed using the heterogenized **HC1** complex, which was shown to be active in recycle reactions and is, therefore, promising for large-scale use.

Heterogeneous MCM-β-diimine nickel complexes are very promising for the oligomerization reactions of ethylene and propylene. One can change the reaction parameters to obtain the desired products.

Acknowledgments

The authors thank CAPES and CNPq for financial support, CNANO UFRGS for the NMR analyses, the CME UFRGS for analysis of the electron micrographs and transmission images, Cristiano Favero for analysis of the adsorption–desorption isotherms, and Isabel Vincent for his help in the propylene gas chromatography analysis.

References

[1] A. Forestière, H. Olivier-Bourbigou, L. Saussine, Oil Gas Sci. Technol. Rev. IFP 64 (2009) 649–667.
[2] A. Kermagoret, R.N. Kerber, M.P. Conley, E. Callens, P. Florian, D. Massiot, F. Delbecq, X. Rozanska, C. Copéret, P. Sautet, J. Catal. 313 (2014) 46–54.
[3] C. delPozo, A. Corma, M. Iglesias, F. Sánchez, Organometallics 29 (2010) 4491–4498.
[4] A. Lacarriere, J. Robin, D. Swierczynski, A. Finiels, F. Fajula, F. Luck, V. Hulea, ChemSusChem 5 (2012) 1787–1792.
[5] M. Lallemand, A. Finiels, F. Fajula, V. Hulea, J. Phys. Chem. C 113 (2009) 20360–20364.
[6] A. Finiels, F. Fajula, V. Hulea, Catal. Sci. Technol. 4 (2014) 2412–2426.
[7] V. Hulea, F. Fajula, J. Catal. 225 (2004) 213–222.
[8] E. Rossetto, M. Caovilla, D. Thiele, R.F. de Souza, K.B. Gusmão, Appl. Catal. A: Gen. 454 (2013) 152–159.
[9] M.O. de Souza, R.F. de Souza, L.R. Rodrigues, H.O. Pastore, R.M. Gauvin, J.M. R Gallo, C. Favero, Catal. Commun. 32 (2013) 32–35.
[10] M.L. Mignoni, M.O. de Souza, S.B.C. Pergher, R.F. de Souza, K.B. Gusmão, Appl. Catal. A: Gen. 374 (2010) 26–30.
[11] V.C. Gibson, S.K. Spitzmesser, Chem. Rev. 103 (2003) 283–315.
[12] A. Kermagoret, P. Braunstein, Dalton Trans. (2008) 822–831
[13] G.P. Belov, P.E. Matkovsky, Petrol. Chem. 50 (2010) 283–289.
[14] M.O. De Souza, R.F. de Souza, L.R. Rodrigues, H.O. Pastore, R.M. Gauvin, J.M.R. Gallo, C. Favero, Catal. Commun. 32 (2013) 32–35.
[15] L.K. Johnson, C.M. Killian, M. Brookhart, J. Am. Chem. Soc. 117 (1995) 6414–6415.
[16] C.M. Killian, D.J. Tempel, L.K. Johnson, M. Brookhart, J. Am. Chem. Soc. 118 (1996) 11664–11665.
[17] D.P. Gates, S.A. Svejda, E. Onate, C.M. Killian, L.K. Johnson, P.S. White, M. Brookhart, Macromolecules 33 (2000) 2320–2334.
[18] S.A. Svejda, L.K. Johnson, M. Brookhart, J. Am. Chem. Soc. 121 (1999) 10634–10635.
[19] C. Bianchini, G. Giambastiani, L. Luconi, A. Meli, Coord. Chem. Rev. 254 (2010) 431–455.
[20] G.C. Vernon, S.K. Spitzmesser, Chem. Rev. 103 (2003) 283–315.
[21] G.J.P. Britovsek, V.C. Gibson, D.F. Wass, Angew. Chem. Int. Ed. 38 (1999) 428–447.
[22] D.S. McGuinness, Chem. Rev. 111 (3) (2011) 2321–2341.
[23] L. Bourget-Merle, M.F. Lappert, J.R. Severn, Chem. Rev. 102 (2002) 3031–3065.
[24] D.J. Mindiola, Angew. Chem. Int. Ed. 48 (2009) 6198–6200.
[25] C.J. Brinker, G.W. Scherer, Sol–Gel Science the Physics and Chemistry of Sol–Gel Processing. San Diego, 1990.
[26] R.A. Sheldon, I.W.C.E. Arends, H.E.B. Lempers, Collect. Czech. Chem. Commun. 63 (1998) 1724–1742.
[27] A.P. Wight, M.E. Davis, Chem. Rev. 102 (2002) 3589–3614.
[28] B. Meunier, Chem. Rev. 92 (1992) 1411–1456.
[29] J.S. Beck, J.C. Vartulli, W.J. Roth, M.E. Leonowicz, C.T. Kresge, K.D. Schmitt, C.T.-W. Chu, D.H. Olson, E.W. Sheppard, S.B. McCullen, J.B. Higgins, J.L. Schlenker, J. Am. Chem. Soc. 114 (1992) 10834–10843.
[30] K.M. Parida, S. Singha, P.C. Sahoo, J. Mol. Catal. A: Chem. 325 (2010) 40–47.
[31] S. Kumari, B. Malvi, A.Kr. Ganai, V.K. Pillai, S. Gupta, J. Phys. Chem. C 115 (2011) 17774–17781.
[32] A.S.M. Chong, X.S. Zhao, J. Phys. Chem. B 107 (2003) 12650–12657.
[33] J. Zhang, H. Gao, Z. Ke, F. Bao, F. Zhu, Q. Wu, J. Mol. Catal. A: Chem. 231 (2005) 27–34.
[34] Y. Li, L. Wang, H. Gao, F. Zhu, Q. Wu, Appl. Organometal. Chem. 20 (2006) 436–442.
[35] M.E. Bluhm, C. Folli, D. Pufky, M. Kröger, O. Walter, M. Döring, Organometallics 24 (2005) 4139–4152.
[36] M.T.N. Villalba, Tese de doutorado, Instituto de Tecnologia de Valência, 1997.
[37] B.J. Hathaway, D.G.J. Holah, J. Chem. Soc. (1964) 2400–2408
[38] M. Kruk, M. Jaroniec, Y. Sakamoto, O. Terasaki, R. Ryoo, C.H. Ko, J. Phys. Chem. 104B (2000) 292–298.
[39] W. Hammond, E. Prouzet, S.D. Mohanti, T.J. Pinnaviam, Micropor. Mesopor. Mater. 27 (1999) 19–25.
[40] M. Kruk, M. Jaroniec, Chem. Matter. 13 (2001) 3169–3183.
[41] J.L. Blin, C. Otjacques, G. Herrier, B.-L. Su, Int. J. Inorg. Mater. 3 (2003) 75–86.
[42] R.F. de Souza, K.B. Gusmão, G.A. Cunha, C. Loup, F. Leca, R. Reau, J. Catal. 226 (2004) 235–239.
[43] S.A. Svejda, M. Brookhart, Organometallics 18 (1999) 65–74.
[44] S.O. Ojwach, I.A. Guzei, L.L. Benade, S.F. Mapolie, J. Darkwa, Organometellics 28 (2009) 2127–2133.
[45] J. Rigoreau, S. Laforge, N.S. Gnep, M. Guisnet, J. Catal. 236 (2005) 45–54.
[46] J. Joni, M. Haumann, P. Wasserscheid, Appl. Catal. A: Gen. 372 (2010) 8–15.
[47] R.M. Enus, S.F. Mapolie, Inorg. Chim. Acta 409 (2014) 96–105.
[48] M.K. Ainooson, S.O. Ojwach, I.A. Guzei, L.C. Spencer, J. Darkwa, J. Organomet. Chem. 696 (2011) 1528–1535.
[49] P.W. Dyer, J. Fawcett, M.J. Hanton, Organometallics 27 (2008) 5082–5087.
[50] P. Prokesová, N. Zilková, S. Mintova, T. Bein, Appl. Catal. A: Gen. 281 (2005) 85–91.
[51] G.S. Nyamato, S.O. Ojwach, M.P. Akerman, J. Mol. Catal. A: Chem. 394 (2014) 274–282.
[52] K. Bouchmella, P.H. Mutin, M. Stoyanova, C. Poleunis, P. Eloy, U. Rodemerck, E.M. Gaigneaux, D.P. Debecker, J. Catal. 301 (2013) 233–241.